Direct fractal measurement and multifractal properties of fracture surfaces

Heping Xie [a], Jin-an Wang [a], E. Stein [b]

[a] *Institute of Fractal Mechanics, Beijing Graduate School, China University of Mining and Technology, Beijing 100083, China*
[b] *Institute of Computation Mechanics, Hannover University, Hannover, Germany*

Abstract

A new method of fractal measurement, the projective covering method (PCM), is proposed in this Letter. Based on the measurements by means of a laser profilometer, the fractal dimension $D \in [2,3)$ of a fracture surface is directly estimated. The projective covering probability function is introduced to systematically analyze the multifractal behavior of the fracture surfaces. © 1998 Elsevier Science B.V.

Keywords: Projective covering method; Fracture surface; Fractal dimension; Multifractal

1. Introduction

Following the introduction of fractal geometry by Mandelbrot [1], many researchers have quantitatively described the roughness of fractured surfaces and also tried to establish the relationship between the fractal dimension and mechanical parameters [2–12].

Extensive experiments and measurement show that, to some extent, fracture surfaces in rocks exhibit a statistical fractal behavior in a certain scale range [3,4]. In fact, understanding of fractal behavior of fracture surfaces advances step by step. Initially, mainly attention was paid to the morphology of fracture surface and one considered a fracture surface a self-similar fractal. The investigations were limited to the measurement of the self-similar fractal dimension [5,6]. Recent studies show that fracture surfaces are not simple self-similar fractals [9,10]. It is impossible, therefore, to describe the roughness of fracture surfaces by using a single fractal dimension [11]. Fracture surfaces display a multifractal behavior.

In general, it is very difficult to perform a direct measurement for a rough surface. Mostly, some indirect methods had to be employed, such as the slit island analysis (SIA) [2], the divider [5,6], and the self-affine varogram [7,11], in measuring of a sectional fracture profile. As a result, fractal dimensions measured by these methods fall in the range $1 < D < 2$. In other words, these methods simplify two-dimensional measurements to one-dimensional ones. Because of the anisotropy and heterogeneity of the fracture surface structure, these measurement do not show a real fractal dimension ($D \in [2,3)$) of the fracture surface. It has been a difficult problem to directly estimate the real fractal dimension for a fracture surface.

To find a solution, a projective covering method is proposed to directly measure the real fractal dimension of fracture surfaces. Additionally, the probability

function of the method is introduced to systematically analyze the multifractal behavior of fracture surfaces.

2. The projective covering method and direct measurement of the fractal dimension of a fracture surface

In order to perform a direct measurement of the fractal dimensions of fracture surfaces, the measurement technique should be taken into account first. Up to now, the techniques developed for measuring of rough surfaces can be classified into mechanical and optical ones. To avoid damages and errors to the measured surfaces caused by scratches of a mechanical probe sliding along the surfaces, an optical technique is commonly used.

The laser profilometer [12], a non-contact optical instrument, is employed in the present study to measure fracture surfaces. Following the principle of triangular reflection, a laser beam released from the source forms a point on the fracture surface. The surface reflects part of the light to a position sensitive detector (PSD) at a certain angle. When the distance between the surface and the light source changes, the reflected light will be thrown to different positions of the PSD. The light-electrical transfer will produce an electronic signal which is proportional to the distance. In this way, the height of a rough surface can be measured. The laser probe LM30 employed in this study is made by Lüneburg Company GmbH, Germany. The measurement range in height is 30 cm, with an accuracy of ±7 μm, and a resolution of 7.5 μm.

In our measurement, a number of fracture surfaces are scanned within an area of 20×20 mm^2 over 6561 points with a digital interval of 0.25 mm. As an example, Fig. 1a shows the morphology of a fracture surface by making use of the laser profilometer.

As is well known, the covering method is one of the most common methods for fractal measurement. It is suitable not only for simple fractals but also for complex fractals [3,4]. However, it appears impossible to use such a method to cover a two-dimensional fractal surface in a direct manner. Some studies have to replace the real fractal dimensions $D \in [2, 3)$ with approximate fractal dimensions $1 < D < 2$ which are obtained from the sectional profile or the SIA method. Based on the topographical data measured by the laser
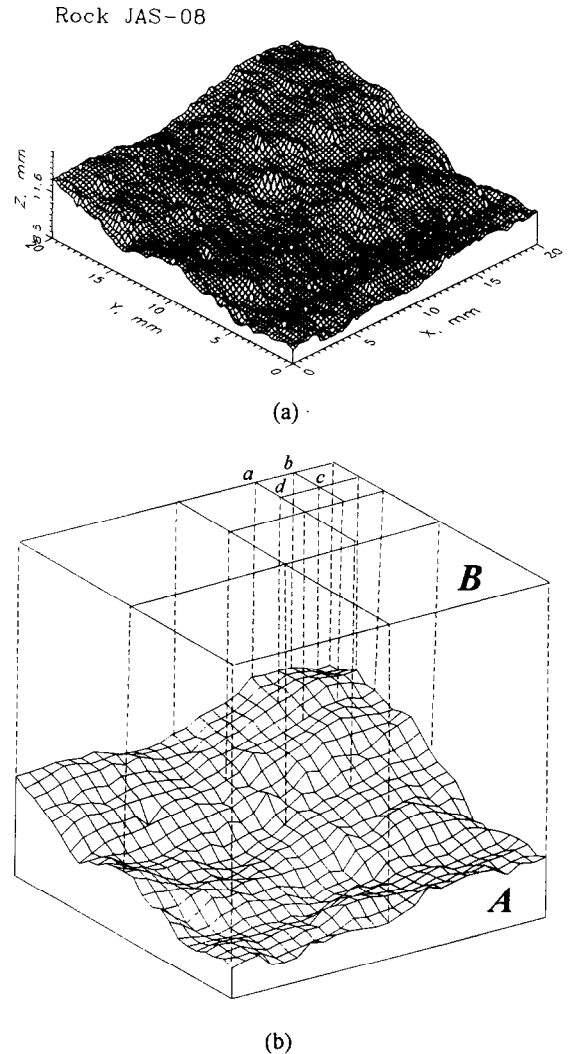

(a)

(b)

Fig. 1. (a) Scanned fracture surface, and (b) the projective covering method.

profilometer, we propose a new method of fractal estimation, the projective covering method (Fig. 1b). By this method, the real fractal dimension $D \in [2, 3)$ for a fracture surface can be directly measured. Symbols A and B in Fig. 1b denote, respectively, a real fracture surface and the corresponding projective framework which covers the surface. When one chooses the kth square $abcd$ (a, b, c, and d are the four points of the square) with a selected scale of $\delta \times \delta$, the laser profilometer can measure the heights at the points a, b, c and d, i.e., h_{ak}, h_{bk}, h_{ck}, and h_{dk}. Accordingly, the area of a rough surface surrounded by points $abcd$ can be
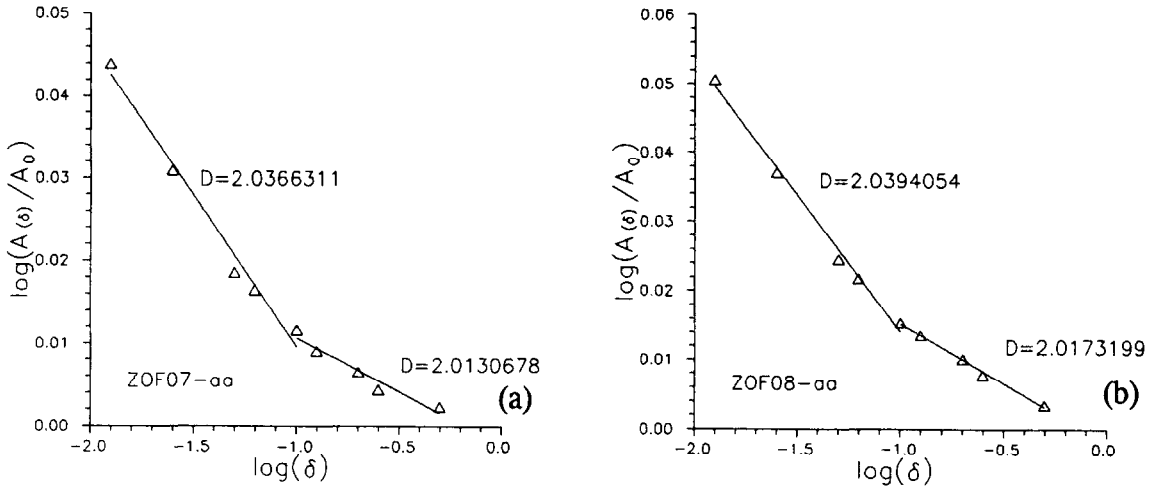
Fig. 2. Estimation of the fractal dimension of a fracture surface by the projective covering method.

approximately calculated by

$$A_k(\delta) = \frac{1}{2}\{[\delta^2 + (h_{ak} - h_{dk})^2]^{1/2}$$
$$\times [\delta^2 + (h_{dk} - h_{ck})^2]^{1/2} + [\delta^2 + (h_{ak} - h_{bk})^2]^{1/2}$$
$$\times [\delta^2 + (h_{bk} - h_{ck})^2]^{1/2}\}. \tag{1}$$

The entire area of the rough surface under the kth scale measurement is given by

$$A_T(\delta) = \sum_{k=1}^{N(\delta)} A_k(\delta), \tag{2}$$

where $N(\delta)$ is the total number of cells in the scale of $\delta \times \delta$ needed to cover the rough surface. The area $A_T(\delta)$ of a rough surface depends on δ. It is clear that, from Eq. (2), a smaller δ yields a greater $A_T(\delta)$. As $\delta \to 0$, $A_T(\delta)$ approximates the real area of the rough surface.

In fractal geometry, the measure of a fractal object in E-dimensional space can be expressed in a general form [4],

$$G(\delta) = G_0\delta^{E-D}, \tag{3}$$

where E represents the Euclidean dimension. This equation can be used for the measurement of a fractal object in the form of either a curve, an area or a volume. For instance, if $E = 1$, then G and δ correspond to a fractal curve. In this case, Eq. (3) becomes

$$L(\delta) = L_0\delta^{1-D}. \tag{4}$$

Similarly, if $E = 2$, G and δ in Eq. (3) correspond to a fractal area, then Eq. (3) yields

$$A_T(\delta) = A_{T0}\delta^{2-D}, \tag{5}$$

where A_{T0} denotes the apparent area of the rough surface. From Eq. (2) and Eq. (5), we have the following relation,

$$A_T(\delta) = \sum_{k=1}^{N(\delta)} A_k(\delta) \sim \delta^{2-D}, \tag{6}$$

where D is the real fractal dimension of the rough surface, i.e. $D \in [2, 3)$.

In the present study, fracture surfaces induced in sandstone by means of indirect tension tests are examined. As shown in Fig. 2 the fractal dimension D of a fracture surface can be directly estimated from the slope β, i.e. $D = 2 - \beta$.

Instead of using a divider of size δ to cover a fracture profile, a projective covering method uses a rectangle of size $\delta \times \delta$ to cover the rough surface. Although this approach is similar to the divider method, it produces a real fractal dimension $D \in [2, 3)$ for a rough surface. In order to verify the projective covering method, comparisons are made between the fractal dimension D_s of the fracture surface and the average fractal dimension of sectional profiles D_x and D_y measured along two orthogonal directions x and y on the same fracture surfaces, and an expected result is produced, i.e.

$$1 + \overline{D_x} \leqslant D_s \leqslant \overline{D_x} + \overline{D_y} \quad \wedge$$
$$1 + \overline{D_y} \leqslant D_s \leqslant \overline{D_x} + \overline{D_y},$$

which has been theoretically proven to be right within the framework of fractal geometry [13,14] (for details see the Appendix).

As shown in Fig. 2, fracture surfaces in rocks do not show *strict self-similar* fractal behavior. The roughness shows the multi-scale fractal property, i.e., the self-similarity is locally defined only. The segmental linearity of the log–log plots in different scale sizes ($\delta = \delta_i/\delta_0$) indicates that a real fracture surface in rock may display multifractality. The fractal dimension depends on the measurement scale of the projective covering network, i.e. the smaller the δ used, the greater the fractal dimension produced, and vice versa.

3. Multifractal behavior of fracture surface

A fracture surface is superimposed by asperities in different orders. However, the distribution of the asperities may spread over a region in such a way that the concentration of asperities varies widely. For instance, a concentration of big asperities is only at a few places, a concentration of small asperities at many places, and a concentration of fine asperities almost everywhere. It can happen that the distribution or measure μ of the roughness displays fractal behavior, and follows a power-law, e.g. $\mu(B_r(x)) \sim r^\alpha$ for a small r, but with a different exponent α from one location to another. The distribution or measure μ with this sort of property is called a *multifractal measure* [13,15]. Multifractals present a move from the geometry of sets as such to geometric properties of the measure. In other words, multifractal measures are related to the study of a distribution of physical or other quantities on a geometric support. Statistical properties of a multifractal structure are characterized by a continuous spectrum of fractal dimension.

Consider a fractal set S consisting of N sample points (any physical quantity underlying measure), and having N_i points in the ith cell. We now introduce the "mass" or *probability* $p_i = N_i/N$ in the ith cell to construct the measure. Notice that the mass in the ith cell of size δ is given by

$$p_i(\delta) = \delta^{\alpha_i}. \tag{7}$$

Here α_i is called the *scaling exponent* (the Lipschitz–Hölder exponent in the classical notion of mathematics), which controls the singularity of the density and may also be called the *exponent of singularity*. A multifractal measure is supported by a set S, which is the union of subsets S_α with α chosen in the continuum of allowed values,

$$S = \bigcup_\alpha S_\alpha. \tag{8}$$

Since the complete set S is fractal, with a fractal dimension D, the subsets have fractal dimensions $f(\alpha) \leqslant D$. For fractal subsets, with a fractal dimension $f(\alpha)$, the number $N(\alpha, \delta)$ of segments of length needed to cover the sets S_α with α in the range α to $\alpha + d\alpha$ is

$$N(\alpha, \delta) = \rho(\alpha)\, d\alpha\, \delta^{-f(\alpha)}. \tag{9}$$

For these sets the measure p_α in a cell of size δ has the power-law dependence, see Eq. (7), on the length scale δ so that we may write $p_\alpha = \delta^\alpha$, and therefore the measure M for the set S given in Eq. (8) may be written [15]

$$M_d(q, \delta) = \int \rho(\alpha)\, d\alpha\, \delta^{-f(\alpha)} \delta^{\alpha q} \delta^d$$
$$= \int \rho(\alpha)\, d\alpha\, \delta^{q\alpha - f(\alpha) + d}. \tag{10}$$

The integral in Eq. (10) is dominated by the terms where the integral has its maximum, in other words for

$$\frac{d}{d\alpha}[q\alpha - f(\alpha)]\,|_{\alpha = \alpha(q)} = 0. \tag{11}$$

Suppose for each q, we have $\alpha = \alpha(q) > 0$, then at $\alpha(q)$

$$q = \frac{df}{d\alpha}(\alpha(q)). \tag{12}$$

Thus, $\alpha(q)$ is the value of α at which the graph of f has slope q. Furthermore, the integral in Eq. (10) can be expressed by [15]

$$M_d(q, \delta) \sim \delta^{q\alpha(q) - f(\alpha(q)) + d}. \tag{13}$$

Here M_d remains finite in the limit $\delta \to 0$ if d equals the mass exponent $\tau(q)$ given by

$$\tau(q) = f(\alpha(q)) - q\alpha(q), \tag{14}$$

where $\alpha(q)$ is the solution of Eq. (11). Thus the mass exponent is given in terms of the Lipschitz–Hölder exponent $\alpha(q)$ for the mass, and the fractal dimension $f(\alpha(q))$ of the set that supported this exponent.

On the other hand, if we know the mass exponents $\tau(q)$, we may determine the Lipschitz–Hölder exponent $\alpha(q)$ (if α is differentiable as a function of q),

$$\frac{d\tau}{dq} = \frac{df}{d\alpha}\frac{d\alpha}{dq} - \alpha - q\frac{d\alpha}{dq}. \tag{15}$$

On putting $\alpha = \alpha(q)$ we get, using Eqs. (15) and (17), that

$$\alpha(q) = -\frac{d}{dq}\tau(q), \tag{16}$$

$$f(\alpha(q)) = q\alpha(q) + \tau(q). \tag{17}$$

Eqs. (16) and (17) give a parametric presentation of the $f(\alpha)$ curve, i.e, the fractal dimension, $f(\alpha)$, of the support of a "singularity" in the measure with Lipschitz–Hölder exponent $\alpha(q)$. The $f(\alpha)$ curve characterizes the measure and is equivalent to the sequence of mass exponents $\tau(q)$. This $f(\alpha)$ is sometimes referred to as the *multifractal spectrum* of the measure μ.

Multifractals can also be expressed in terms of the generalized dimension function [1,4],

$$D_q = \frac{1}{q-1}\lim_{\delta\to 0}\frac{\log\sum p_i^q(\delta)}{\log\delta}. \tag{18}$$

The moment order q is any number in the range $-\infty$ to $+\infty$, and the function D_q is the *spectrum* of *fractal dimension* for a fractal measure on the set S. Choosing large values of q ($q \gg 1$) in Eq. (9) favors contributions from cells with relatively high values of p_i; conversely, $q \ll 1$ favors the cells with relatively low values of the measure p_i on the cell.

Chhabra and Jensen [16] proposed a method for the calculation of $f(\alpha)$. On the basis of box covering, they constructed a uniformed parametric measure $\mu(q,\delta)$,

$$\mu(q,\delta) = \frac{[p_i(\delta)]^q}{\sum_i[p_i(\delta)]^q}, \tag{19}$$

where $\sum_i[p_i(\delta)]^q$ indicates the summation with q exponent order of the probability for all boxes. The Hausdorff dimension of the subsets is given by

$$f(\alpha) = \lim_{\delta\to 0}\frac{\sum_i \mu_i(q,\delta)\log\mu_i(q,\delta)}{\log\delta}. \tag{20}$$

The average value on the singularity intensity of the measure $\alpha_i = \log p_i/\log\delta$ can be approximated by

$$\alpha(q) = \lim_{\delta\to 0}\frac{\sum_i \mu_i(q,\delta)\log p_i(\delta)}{\log\delta}. \tag{21}$$

Therefore, for each given q value, the corresponding $\alpha(q)$ and $f(\alpha)$ can be calculated through Eqs. (19)–(21), and the $f(\alpha)$-$\alpha(q)$ curve can be produced.

On employing the projective covering method, the projective covering probability is defined as

$$p_i(\delta) = \frac{A_i(\delta)}{\sum_j A_j(\delta)} = \frac{A_i(\delta)}{A_T(\delta)}, \tag{22}$$

where $A_i(\delta)$ is the area in the ith cell with the scale size of δ, and $A_T(\delta)$ is the total area of the fracture surface which is measured under the scale of δ (Eqs. (1) and (2)). Therefore, the probability $p_i(\delta)$ varies with the scale of δ, and it manifests different orders of asperities on a rough fracture surface for different δ. According to Eqs. (19)–(22), $f(\alpha)$ and $\alpha(q)$ are calculated for different exponent orders q.

As an example, Fig. 3a shows the $f(\alpha)$-$\alpha(q)$ curve which is based on the measurement of a tensile fracture surface in sandstone. As shown, $f_{max}(= 2.0)$ occurs at $q = 0$, i.e. $df/dq|_{\alpha=0} = 0$. This is an expected result since the support of the measure (the cell used to cover the surface) is a plane, which is two dimensional. $f(\alpha)$ decreases to a non-zero value as the exponent order $q \to -\infty$, whereas $f(\alpha)$ approaches 0 as $q \to +\infty$. This indicates that a fracture surface displays different fractal characters in a varying range of q.

From Eq. (18), the D_q-q curve is calculated and presented in Fig. 3b. It shows that the fractal dimension D_q increases with the increase of absolute values q ($q < 0$), and may achieve a constant maximum when $q \to -\infty$. As mentioned previously, for $q > 0$, a greater q emphasizes the contribution from cells with relatively high values of p_i, and in this case, the fractal dimension D_q describes mainly the *rougher* asperities on the fracture surface. Conversely, for $q < 0$, a greater value of $|-q|$ favors the cells with relatively low values of p_i, and D_q now mainly describes the *smooth* asperities on the fracture surfaces. We will see later that the spectrum of D_q in the range $q > 0$ can be a diagnostic parameter to distinguish fractures of
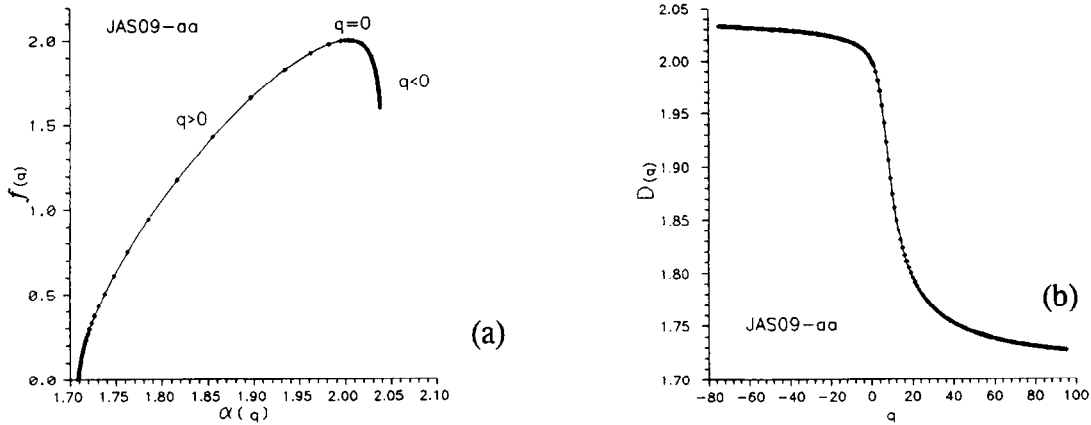
Fig. 3. Multifractal spectrum of a fracture surface in sandstone.

rock which have different fracture mechanisms and strengths.

Figs. 4a,b show the $f(\alpha)-\alpha(q)$ and D_q-q curves for extended fracture surfaces included in sandstones which have different tensile strengths. In general, the fracture surface in rocks which has a relatively low tensile strength shows a wider range of $f(\alpha)$ spectrum with reference to q, and lower D_q ($q < 0$) or higher D_q ($q > 0$). However, there exist occasional cases which destroy the proportional relationship between σ_T and D_q. It might be influenced by some other structural factors or mechanical parameters which should be investigated.

Figs. 4c,d show a few $f(\alpha)-\alpha(q)$ and D_q-q curves for shear fracture surfaces induced in sandstones by means of conventional triaxial compression tests, where $(\sigma_1 - \sigma_3)_{max}$ indicates the maximum differential stress the sandstones underwent, and the confining stress $\sigma_2 = \sigma_3 = 10$ MPa. Although there is a negative difference in D_q when $q < 0$, the significant difference in the appearance of $f(\alpha)$ and D_q can be found in the full range spectrum for different $(\sigma_1 - \sigma_3)_{max}$. As shown, the greater the $(\sigma_1 - \sigma_3)_{max}$, the narrower the range of $f(\alpha)$ and the bigger the drops in D_q for $q > 0$.

In comparison with the multifractal spectrum of fracture surfaces induced by different fracture mechanisms (Figs. 4e,f), the spectrum for an extension fracture surface displays a wider range of $f(\alpha)$ and greater values of D_q ($q < 0$). On the contrary, the spectrum for a shear fracture surface shows a narrower

range of $f(\alpha)$ and smaller values of D_q ($q < 0$), and for hybrid fracture surfaces, the multifractal spectrum ranges between those for the extension and shear fracture surfaces.

Rather than a single fractal, a multifractal fracture provides more characteristics and much information about the concentration distribution of the variables under investigation. However, we have said little about the physical meaning of the $f(\alpha)-\alpha(q)$ and D_q-q curves; indeed, there are considerable problems associated with their interpretation. For instance, the meaning of $f(\alpha) < 2.0$ and $D_q < 2.0$ ($q > 0$) for a fracture surface which has been believed to have a theoretical fractal dimension $D \in [2,3)$. An extended study really is needed to cover the particular subject; this has been beyond the scope of the present work.

4. Conclusions

In this Letter, a new measurement method, the projective covering method, is proposed, which makes it possible to cover a two-dimensional fractal object for a direct estimation of the real fractal dimensions $D \in [2, 3)$ for fracture surfaces. The probability function of the surface roughness is constructed for the analysis of a fracture surface within the framework of multifractal theory. The multifractal behavior of natural fracture surfaces in rocks has been investigated. Besides the general relationship between the tensile strength of rocks and fractal dimensions of rock fracture surfaces (σ_T is inversely proportional to D), the
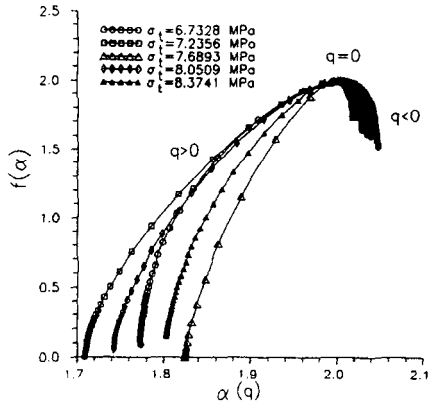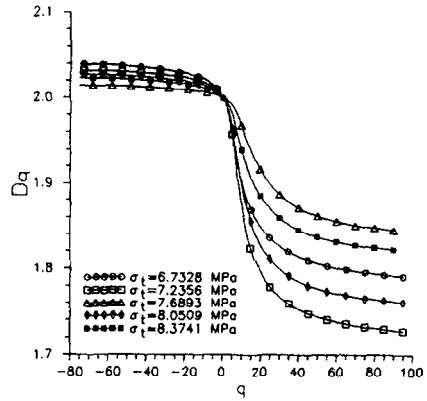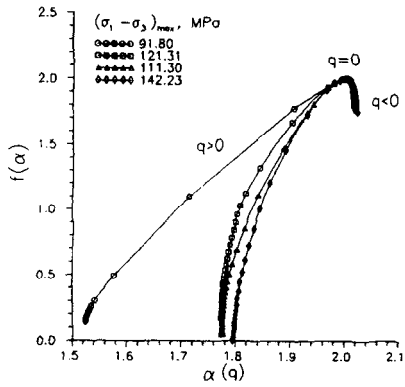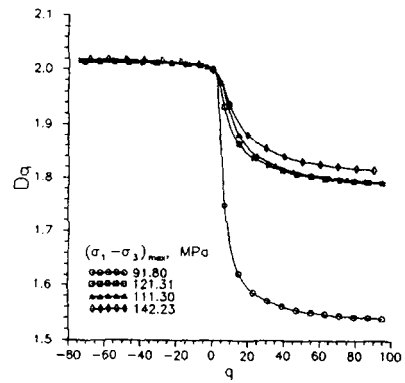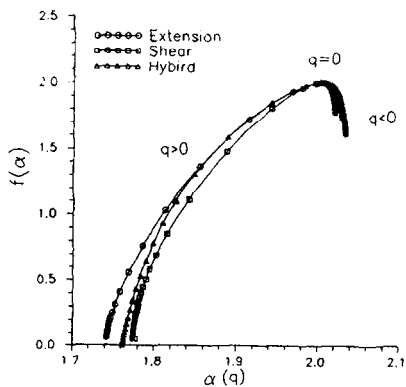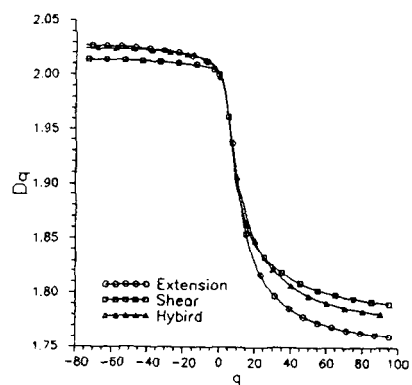
Fig. 4. Multifractal behavior of rock fracture surfaces under different loading conditions.

multifractal spectrum could yield much more information on the fracture mechanism, which is helpful in understanding the structural phenomenon of fracture surfaces.

Acknowledgement

Appendix A. Verification

To verify the projective covering method, for the same fracture surfaces, the fractal dimensions along individual profiles in the x and y directions, respectively, are measured by a divider method. As is well known, the fractal dimension for a profile is calculated by

$$L(\delta) = L_0 \delta^{1-D}.$$

Here, L_0 is the apparent length of the profile, $L(\delta)$ is the length of the profile measured under the scale δ ($\delta = \delta_i/\delta_0$, δ_i is the span of the divider at the ith measurement). The fractal dimension measured in this way has the values $D \in [1,2)$ for a single profile. In order to compare the fractal dimension of a fracture surface with that measured from profiles, let us elaborate, first of all, the dimension formulae of the Cartesian product of fractal sets.

Suppose E is a subset of $\mathbb{R}^n$ and F is a subset of $\mathbb{R}^m$; the *Cartesian product*, $E \times F$, is defined as the set of points with first coordinate in E and second coordinate in F, i.e.

$$E \times F = \{(x, y) \in \mathbb{R}^{n+m} : x \in E, y \in F\}. \quad (A.1)$$

Thus, if E is a unit interval in $\mathbb{R}$, and F is a unit interval in $\mathbb{R}^2$, then $E \times F$ is a unit square in $\mathbb{R}^3$ (Fig. A.1). In such a case, it is obvious that

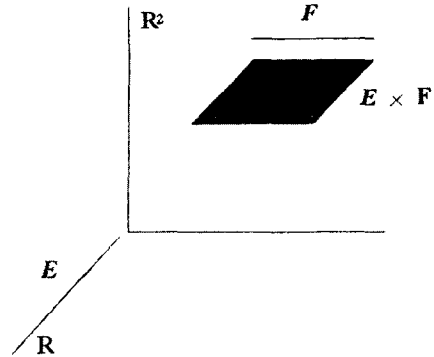$$\dim(E \times F) = \dim E + \dim F, \quad (A.2)$$

Fig. A.1. The Cartesian product of a unit interval in $\mathbb{R}$ and a unit interval in $\mathbb{R}^2$ (from Ref. [13]).

using the classical definition of dimension. This holds more generally, in the "smooth" situation, where E and F could be smooth curves, surfaces or high-dimensional manifolds. However, Eq. (A.2) is not always valid for "fractal" dimensions. For fractal dimensions, the most general result possible is an inequality [13]

$$\dim(E \times F) \leqslant \dim E + \dim F. \quad (A.3)$$

For simplicity, take $E \subset \mathbb{R}$ and $F \subset \mathbb{R}$. Choose the number $s > \dim E$ and $t > \dim F$. Then there is a number $\delta_0 > 0$ such that E may be covered by $N_\delta(E) \leqslant \delta^{-s}$ intervals, and similarly, F may be covered by $N_\delta(F) \leqslant \delta^{-t}$ intervals of side length δ for all $\delta \leqslant \delta_0$. Thus, $E \times F$ is covered by $N_\delta(E)N_\delta(F)$ squares formed by products of these intervals with length δ, so that

$$N_\delta(E \times F) = \delta^{-\dim(E \times F)} = N_\delta(E) \times N_\delta(F)$$
$$\leqslant \delta^{-s}\delta^{-t} = \delta^{(-s+t)}. \quad (A.4)$$

Recall that $s > \dim E$ and $t > \dim F$, and Eq. (A.4) follows. By choosing s and t equal to $\dim E$ and $\dim F$, the equality holds in Eq. (A.4).

For example, a Koch fractal surface as shown in Fig. A.2 is constructed by producing a Koch curve with a straight line perpendicular to the Koch curve. As is well known, the "fractal" dimension for a straight line is 1 and the fractal dimension for Koch curve is $D = 1.2619$. Following Eq. (A.4), the product yields $D_2 = 1 + 1.2169 = 2.2169$ for a Koch fractal surface.

For a real fracture surface in rock, the roughness varies from profile to profile and from one direction
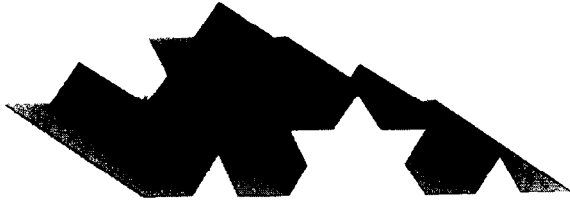
Fig. A.2. Koch fractal surface formed by the product of a Koch curve with a straight line.

to another [14]. In order to clarify the fractal dimension along different directions, the fractal dimensions of profiles within the fracture surfaces are measured by the divider method along the x and y directions, respectively. The interval of each profile scanned by a laser profilometer is 0.25 mm. The fractal dimension is estimated in two orthogonal directions, respectively, by the following equations,

$$L_x(\delta) = L_{x0}\delta^{1-D_x}, \quad L_y(\delta) = L_{y0}\delta^{1-D_y}, \quad (A.5)$$

where $L_x(\delta)$ and $L_y(\delta)$ are the real profile lengths in the x and y directions measured under the scale of δ_i by the divider method, and D_x, D_y are fractal dimensions estimated along the x and y directions, respectively. Investigation [14] shows that the fractal dimensions of the profiles on the surface are locally concentrated, but dispersed spatially over the entire surface. From this point of view, the fractal dimension obtained by averaging of the fractal dimensions of all profiles represents a statistical fractal property.

To compare the results of the productive covering method with divider method, the fractal dimension for a rough surface is next calculated as follows,

$$D_{xy} = \frac{1}{N} \sum_{i=1}^{N} (D_{x_i} + D_{y_i}). \quad (A.6)$$

The results are given in Table A.1, where D_x and D_y are the average values of the fractal dimensions which are estimated by the divider method over 81 scanning profiles in the x and y directions, respectively; D_{xy} ($= D_x + D_y$) is the averaged fractal dimension of profiles over the rough surface; and D_s is the fractal dimension estimated by the direct projective covering method. By comparison, D_s is slightly smaller than D_{xy}, (see Table A.1). The results can be expressed as follows,

Table A.1

Fractal dimensions of rock fracture surfaces. D_x, D_y are the average fractal dimensions estimated by the divider method for the profiles in the x, y direction; D_{xy} is the summation of D_x and D_y ($D_{xy} = D_x + D_y$), and D_s the fractal dimension directly estimated by projective covering methods

No.	Sample	D_x	D_y	D_{xy}	D_s
1	JAS01-aa	1.02620	1.018331	2.044531	2.042013
2	JAS02-aa	1.044379	1.034598	2.078977	2.0742193
3	JAS03-aa	1.043866	1.0301864	2.0740524	2.0708306
4	JAS04-aa	1.065890	1.046345	2.112235	2.100897
5	JAS05-aa	1.0509943	1.0366843	2.0876786	2.0818937
6	JAS06-aa	1.0398555	1.0269191	2.0667746	2.064701
7	JAS07-aa	1.048658	1.0313137	2.0799717	2.0734053
8	JAS08-aa	1.0492081	1.034011	2.0832191	2.0770266
9	JAS09-aa	1.0588974	1.0418709	2.1007683	2.0824751
10	JAS10-aa	1.039661	1.0265146	2.0634096	2.063206
11	JAS11-aa	1.0486502	1.0328192	2.0814694	2.0736565
12	JAS12-aa	1.0538008	1.0394035	2.0932043	2.080631
13	ZOF05-aa	1.0251804	1.0216661	2.0468465	2.0437931
14	ZOF07-aa	1.0274177	1.0186337	2.0460514	2.0421595
15	ZOF08-aa	1.0269127	1.0187078	2.0456205	2.0434385
16	STA-P41	1.0346635	1.0216785	2.056342	2.0559967
17	J1-599B	1.0581690	1.0325522	2.0907212	2.0815781
18	J2-599R	1.069016	1.0336108	2.1026268	2.0865448
19	ZOF03	1.0458004	1.0295378	2.0753382	2.0709635

$$1 + \overline{D_x} \leqslant D_s \leqslant \overline{D_x} + \overline{D_y} \quad \wedge$$
$$1 + \overline{D_y} \leqslant D_s \leqslant \overline{D_x} + \overline{D_y}, \quad (A.7)$$

which agree very well with reference to Eq. (A.4). This leads to the conclusion that the projective covering method yields a quite satisfactory result in a direct manner to estimate the fractal dimension of fracture surfaces in rocks.

References

[1] B.B. Mandelbrot, The Fractal of Nature (Freeman, New York, 1982), p. 468.

[2] B.B. Mandelbrot, Fractal Character of Fracture Surface of Metals, Nature (London) 308 (1984) 721.

[3] H. Xie, W.G. Pariseau, Science in China (Series B), 37 (1994) 1269.

[4] H. Xie, Fractals in Rock Mechanics (Balkema, Rotterdam, Brookfield, 1993), p. 453.

[5] J.R. Carr, J.B. Warriner, Bull Assoc. Eng. Geol. 24 (1989) 253.

[6] Y.H. Lee, J.R. Carr, D.J. Barr, C.J. Haas, Int. J. Rock Mech. Min. Sci. Geomech. Abstr. 127 (1990) 453.

[7] S.L. Huang et al., Int. J. Rock Mech. Min. Sci. 29 (1992) 89.

[8] C.Y. Poon et al., J. Phys. D: Appl. Phys. 25 (1992) 1269.

[9] S.M. Miller, P.C. McWilliams, J.C. Kerkering, in: Proc. 31th U.S. Symp. Rock Mech., eds. W.A. Hustrulid, G.A. Jonhson, (Balkema, Rotterdam, 1990), p. 471.

[10] N.E. Odling, Rock Mech. Eng. 27 (1994) 135.

[11] J.A. Wang, H. Xie, M.A. Kwaśniewski, J. China Coal Sci. 1 (1996) 16.

[12] M.A. Kwaśniewski, J.A. Wang, in: Géotechnique et Environnement, eds. J.P. Piguet, F. Homand, Vandœvre-lès-Nancy, Sciences de la Terre, 1993, p. 163.

[13] K. Falconer, Fractal Geometry, Mathematical Foundations and Applications (Wiley, Chichester, 1990), p. 288.

[14] J.A. Wang, On Fractal Characterization of Rock Fracture Surface, Post Doctoral Thesis, China University of Mining and Technology, Beijing, (1997).

[15] J. Feder, Fractals (Plenum, New York, 1988), p. 383.

[16] A. Chhabra, R.V. Jensen, Phys. Rev. Lett. 62 (1989) 1237.